Viswanath, R.N.; Weissmueller, J.:

Electrocapillary coupling coefficients for hydrogen electrosorption on palladium

In: Acta Materialia (2013) Elsevier

DOI: 10.1016/j.actamat.2013.07.013

Electrocapillary Coupling Coefficients for Hydrogen Electrosorption on Palladium

R.N. Viswanath[1,2,*] and J. Weissmüller[2,3]

[1] Surface and Nanoscience Division, Materials Science Group, Indira Gandhi Centre for Atomic Research, Kalpakkam, India

[2] Institut für Werkstoffforschung, Werkstoffmechanik, Helmholtz-Zentrum Geesthacht, Geesthacht, Germany

[3] Institut für Werkstoffphysik und Werkstofftechnologie, Technische Universität Hamburg-Harburg, Hamburg, Germany

* E-Mail for correspondence: rnv@igcar.gov.in

The surface stress *f*, a capillary force at solid surfaces, has important implications for the behavior of nanomaterials. Surface stress is known to vary considerably when atoms adsorb on the surface, yet the underlying mechanisms are poorly understood. Our in-situ dilatometry study of H adsorption on porous nanocrystalline Pd provides quantitative data for the response of *f* to changes in the adsorbate coverage. The porous body is immersed in aqueous electrolyte and H adsorption controlled and measured electrochemically. The surface stress response is quantified by means of the electrocapillary coupling parameter, ς, defined as the derivative of *f* with respect to the superficial charge density. The results support previous, more indirect findings for ς. We show that ς is precisely predicted by a model based on the continuum mechanics of superficial layers containing misfitting solute.

Introduction

The surface stress, *f*, at the surface of a solid needs to be balanced by counteracting stresses in the bulk [1]. In materials with a nanoscale microstructure, the ensuing, surface-induced bulk stresses can be large and they may have important ramifications for the material's behaviour. Among the consequences are considerable modifications of magnetic [2] and alloy phase diagrams [3] as well as shear instabilities that impose lower limits on the size of stable nanoscale objects or microstructures [4,5,6]. Surface stresses undergo large variation when the state of the surface is changed, for instance by adsorption of atoms from gas or of ions from solution, or by electric charging [7,8]. These phenomena are of practical importance in cantilever-based sensing schemes [9,10,11] and in actuators driven by changes of the electrode potential in electrolyte [12,13,14] or of the chemical potential in gas [15]. While the response of *f* to adsorption or to electric charging can be computed by *ab initio* density functional theory in good agreement with experiment [16,17,18], we still lack a predictive theory connecting the observations from real-world or computer experiments to simple concepts for the interaction between adsorbate atoms or electric charging with the host material. Here, we explore the variation of the surface stress of Pd during the adsorption of H from electrolyte, and we show that the response of *f* to adsorption can be quantitatively understood in terms of the known interaction parameters of H interstitial atoms in bulk Pd.

Electrochemical studies can provide particularly detailed and precise information on the surface stress variation during changes of state at the solid surface [7,8]. A key observable in such experiments is the electrocapillary coupling parameter ς, defined by $\varsigma = \mathrm{d}f/\mathrm{d}q|_e$ where q and e denote, respectively, the superficial charge density and the tangential strain at the surface. The value of ς varies with the electrode potential, and is characteristic for the acting electrode process. For instance, ς values reported for Pt have opposite sign for adsorption of hydrogen and adsorption of oxygen species [19].

A specific example for the significance of the electrocapillary coupling strength is the catalytic activity of compositionally graded surfaces, for instance in core-shell catalyst particles. Here, the catalytically active material is enriched in the surface layer of atoms and so does not, in general, see the same interatomic spacing as in its elemental crystalline state. Besides changes in the electronic structure of the surface due to alloying or electron exchange with the substrate material, the change in interatomic spacing or, in other words, the elastic strain, at the surface contributes to changing adsorption enthalpies and, thereby, the catalytic activity [20,21,22,23]. It has been pointed out that studies of the electrocapillary coupling allow to isolate the contribution of the mechanics and to quantify its impact on adsorption [18]. The strategy rests on a Maxwell equation that equates $\mathrm{d}f/\mathrm{d}q|_e$ to the derivative of electrode potential, E, with respect to e. Simple models of electrosorption then suggest a relation to the molar enthalpy, h^{ad}, of adsorption. The relevant equalities for ς can be summarised by [18]

$$\varsigma = \left.\frac{\mathrm{d}f}{\mathrm{d}q}\right|_e = \left.\frac{\mathrm{d}E}{\mathrm{d}e}\right|_q = -\frac{1}{zF}\left.\frac{\mathrm{d}h^{\mathrm{ad}}}{\mathrm{d}e}\right|_\Gamma , \qquad (1)$$

where z, F and Γ denote, respectively, valency, Faraday constant, and specific excess of adsorbate.

Because of their many surfaces, nanoporous materials afford a sensitive measurement of the surface stress. In a previous study [18], it was shown that $\mathrm{d}f/\mathrm{d}q|_e$ for Pd – as measured on porous nanocrystalline (pnc-) Pd – indeed agrees with the strain-derivative of the potential for H electrosorption on pseudomorphic monolayers as reported in Ref. [22]. The similarity of the experimental ς-value reported to that for the deposition of ≤ 1 monolayer of H (underpotential deposition, UPD) on Pt supported the conclusion. Yet, the confirmation lacked stringency, because no conclusive separation was achieved between, on the one hand, the UPD of a H adsorbate layer on the Pd surface and, on the other hand, H absorption

in the bulk of the Pd nanoparticles. In fact, a recent surface stress study of H electrosorption on thin films of Pd emphasizes that H is absorbed in the bulk at an early stage of the electrosorption process [24].

The alloying of H into bulk Pd has been studied in great detail [25, 26], and several studies explore H in Pd nanoparticles. Early work pointed out an enhanced solubility of H in dilute nanoscale Pd-H, along with a narrowed miscibility gap [27, 28, 29, 30]. This can be traced back to enrichment and depletion at the surface as well as the elastic interaction of H in the bulk with stresses originating from the capillary forces [31]. It was also shown that H adsorbed on nanoclusters is at least partly incorporated in subsurface sites [28].

Here, we revisit the issue of electrocapillary coupling at Pd surfaces in the H electrosorption regime. We explore the surface stress of pnc-Pd electrodes by in-situ dilatometry and discuss the signatures of H adsorption in terms of the continuum theory of elasticity of alloys. We present a continuum model of H interaction with the surface and the bulk of Pd that allows us to identify the distinctive signatures of both processes in experiment, and to confirm the earlier results for ς from Ref. [18].

Experimental details

Pd nanoparticles were produced by the inert gas condensation (IGC) method [32, 33], using thermal evaporation of Pd in a ultra-high vacuum environment back-filled with He (6N purity and 250-300 Pa pressure). Procedures were identical to those of Ref. [31], except that the die-and-anvil, *in situ* consolidation of the particles used a low compaction pressure (~1 MPa) so as to create a porous electrode, rather than the nearly full density compacts that are produced in the more conventional IGC studies. Porous samples were cylindrical, 1.5 mm in diameter and 1.8 - 2 mm in length.

A commercial Pd foil (Alfa Aesar®, 99.99% purity) of 1cm^2 area and thickness 25 µm was used for the reference measurements on planar surfaces.

X-ray powder diffraction in Bragg-Brentano geometry was used to determine the mean crystallite size, L. The Bragg reflection broadening was evaluated using a modified Williamson-Hall algorithm and the procedures of Ref. [34] (including the software CGSize available as supporting online material of that reference), assuming Cauchy size and Gauss strain broadening and correcting for instrumental broadening.

Details of the in-situ dilatometry experiments are reported elsewhere [19, 35]. In brief, a miniaturized electrochemical cell, placed in the sample space of a dilatometer [Netzsch® 402C], contains two pnc-Pd samples serving as the working and counter electrodes as well as a Ag/AgCl/3M KCl reference electrode (World Precision Instruments, Inc.) with low leakage (5.7 x 10^{-8} mL/hr). A bath thermostat controlled the temperature at 283 ± 0.1 K. The linear strain, ε, is defined as the length change, Δl, normalized to the length, l_0, in an arbitrary but fixed reference sate, $\varepsilon = \Delta l / l_0$.

Glassware was routinely cleaned with oxidizing acid (H_2SO_4/H_2O_2) and rinsed with 18.2 MΩ cm grade water. The electrolyte was 0.7 M NaF solution with a pH value of 8.5. The potential was controlled by a potentiostat (PGSTAT 100, EcoChemie), and cyclic voltammetry used the linear scan mode, typically at scan rate 1 mV/s. The net charge transferred, δQ to the electrode during cyclic potential scans was determined by integration of the electrode current.

Prior to the in-situ studies in NaF solution, the Pd electrodes were immersed in 0.1 M H_2SO_4 and underwent repeated electrochemical cycling in oxidation/reduction intervals $-0.25\ \text{V} < E < 0.75\ \text{V}$. The pre-treatment is essential for reproducible results [19,35].

Results

Figure 1 shows x-ray powder diffraction data of pnc-Pd and a modified Williamson-Hall graph based on data for the reflection full width at half maximum. The data exhibits straight-line behaviour, suggesting that the evaluation provides a valid separation of grain size and microstrain [34]. The slope of the straight line of best fit implies the mean crystallite size L = 11.1±0.7 nm. Approximating the particles as spheres we obtain the mass-specific surface area α_m as $6 / L \rho$ with ρ the mass density of bulk Pd, 12.023 g/cm^3. The estimated value emerges as $\alpha_m = 43$ m^2/g.

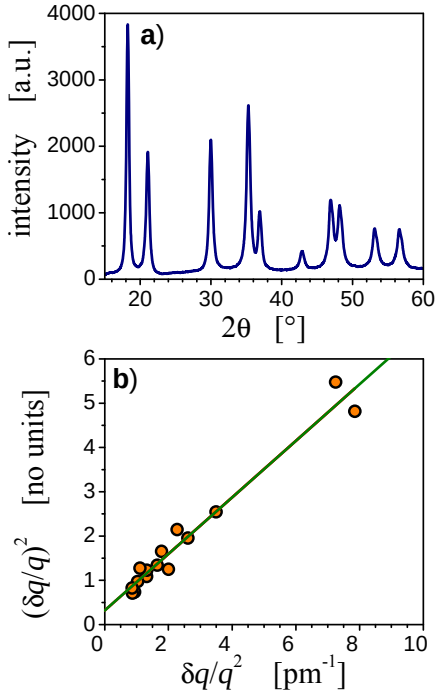

Figure 1. X-ray diffraction results for porous nanocrystalline pnc-Pd. **a)** Powder diffractogram of intensity vs. scattering angle 2θ. b) Modified Williamson-Hall plot. Grain size is determined from slope of straight line of best fit.

We now inspect in situ dilatometry results for potential scans in different potential regions, and start out with a region covering the ad- and absorption of hydrogen as well as oxidation/reduction. Figure 2 displays the electrochemical and mechanical signatures of six successive cyclic scans. Because of the excellent agreement, the separate graphs superimpose and are not resolved in the figure. This supports the sensitivity and reproducibility of the in-situ dilatometry technique.

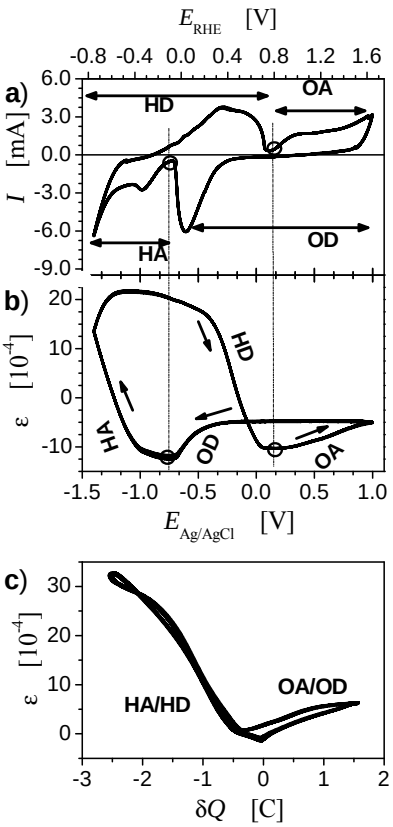

Figure 2. Results of in-situ dilatometry in the potential interval –1.4 to 1.0 V. (a) Cyclic scans of current I vs. electrode potential E. (b) Strain ε vs. E. (c) ε vs. charge δQ. The arrows in (a) provide a rough indication of hydrogen adsorption and absorption (HA), hydrogen desorption (HD), oxidation or adsorption of OH^- (OA) and reduction or desorption of OH^- (OD) regimes. The potential at which δQ = 0 is chosen arbitrary.

Figure 2a) shows cyclic voltammograms (CVs) of current I versus the electrode potential E during cyclic potential scans. The potential regions of the dominant electrochemical processes – namely the electrosorption of H and of OH species – are indicated in the figure. Figure 2b) shows the corresponding dilatometry data, measured simultaneously with the CV. It can be seen that the onset of each adsorption or desorption process is reflected by breaks in the graph of strain, ε, versus E. As in our previous dilatometry study of Pt [19], the onset of hydrogen electrosorption coincides with the end of OH-desorption, and similarly, the onset of the OH-adsorption coincides with the end potential for hydrogen desorption. These features are supported by signatures in the CV and in the dilatometry. The hysteresis of both electrosoprtion processes is noteworthy. The two hysteretic segments overlap around the centre of the measurement scan, so that no double layer region is observed in the CV.

Figure 2(c) shows ε plotted versus the net charge, δQ, transferred to the electrode. The potential at which δQ = 0 is chosen arbitrarily. Contrary to the graph of strain versus potential, the plot of strain versus the charge is almost free of hysteresis. Furthermore, the graph exhibits roughly linear segments with differently signed slopes during hydrogen and oxygen species electrosorption.

In Fig. 2b) it is noteworthy that the graphs are closed, indicating that the transferred charge – and, thereby, the electrosorbed H – can be completely recovered, as in an ideal, pseudocapacitive process. Note that the CV of Fig. 2a) near its cathodic vertex resembles that of a Faraday reaction inasmuch as the negative- and positive-going branches of the $I(E)$ graph coincide. Yet, the finding of recoverable charge rules out noticeable Faraday reactions. It is then natural to assume that the current near the negative potential vertex is the signature of absorption of H into the bulk of the nanograins. Coinciding cathodic and anodic branches of $I(E)$ are here indicative of transport-limited absorption and a failure to reach saturation. It is also natural to assume that hydrogen will also adsorb at the surface. The processes of absorption and adsorption will be considered in more detail in the discussion, see below.

The hysteresis in the variation of current and strain with potential is partly due to potential gradients in the electrolyte within the pore space. This is apparent when Figs. 3a) and 3b) are compared. The former displays a CV on the planar Pd surface of a conventional, massive polycrystalline Pd sheet electrode, whereas the latter is for pnc-Pd. In the respective CVs, the analogous electrochemical features are observed at quite different potentials, with the hysteresis noticeably larger in the porous sample. However, in relation to the in-situ data for pnc-Pd it is noted that the dilatometer recorded the strain simultaneously with the voltammogram. Therefore, the correlation between the respective features is forceful and unambiguous.

As compared to Fig. 2, the electrochemical in-situ dilatometry experiments of Fig. 3b)-d) have a more positive cathodic vertex potential (-1.05V), including the first current peak in the hydrogen electrosorption regime but excluding most of the presumed H absorption current. The data thereby emphasizes the initial part of the H electrosorption regime of Fig. 2 where, upon close inspection of Fig. 2c), a small region with lesser slope of ε versus Q is perceived. By inspection of the CV's it is also seen that the negative-going scan of Fig. 3b) ends after a peak in the CV at E ~ -950mV. This peak corresponds to a similar feature in the CV of the planar Pd surface. In view of literature results on Pd (111) surfaces [24, 36] the aforementioned peak can be attributed to H UPD.

Figure 3c) displays charge transfer, δQ, versus E. As above, the graph is closed, supporting that the charge can be recovered. Figure 3d) shows the strain plotted versus δQ. Similar to the results of Fig. 2c), the plot of ε versus δQ exhibits little hysteresis, suggesting that the measured strain ε is a function of δQ.

When Pd is repeatedly cycled in the potential interval between the onset of oxygen species adsorption during positive-going scans and of H UPD during negative-going scans, i.e., between –0.5 V and –0.2 V, one obtains a featureless CV that is free of electrosorption features. We focus on this condition of the electrode as our third potential interval of study. Even though anion adsorption cannot be ruled out on Pd, the conditions may approximate capacitive double layer charging.

Figure 4a) shows 6 CVs superimposed. The successive CVs are again practically identical. Their lack of feature is at least compatible with dominantly capacitive charging. The net charge transferred δQ and the simultaneously measured strain, 4b) and 4c), are also featureless. Figure 4d) shows ε versus surface charge δQ. The variation of strain with charge is linear and free of hysteresis. It shows the electrode to ex-

pand with positive charging, in agreement with the reported in-situ strain results of Au [37, 38] and Pt [19] in aqueous electrolytes.

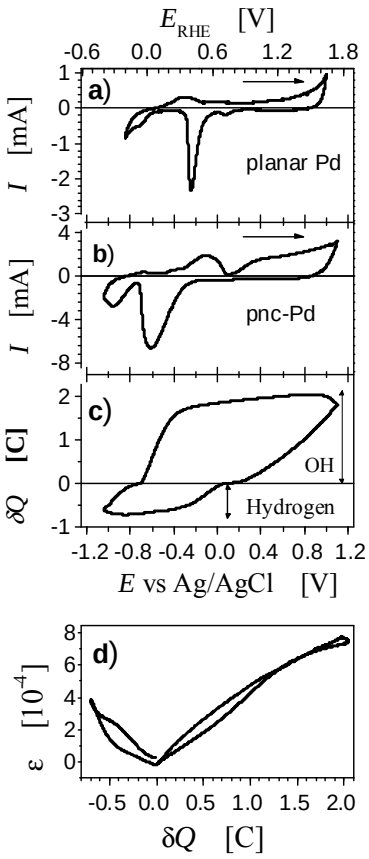

Figure 3. Results of cyclic voltammogram for (a) planar Pd and (b) for pnc-Pd in NaF (0.7 M) electrolyte. Figure (c) displays the charge δQ obtained from the cyclic scan of figure 2b. (d) ε vs. charge δQ. The potential at which $\delta Q = 0$ is chosen arbitrary.

Discussion

The key results of the present study are data for the strain versus the potential or versus the superficial charge density for porous nanocrystalline pnc-Pd, with an emphasis on the variation during H electrosorption. The phenomenology is closely similar to our findings for electrosorption on Pt, see Ref. [19]. In relation to hydrogen electrosorption, the data shows indications of both, hydrogen UPD on the surface and hydrogen absorption in the bulk of the nanograins. Yet, the separation of adsorption and absorption is not obvious. As a prerequisite for discussing the issue we shall start out by inspecting the surface area and the implications for apparent hydrogen coverage.

Surface area and H coverage

Near their negative vertex, the CVs in the potential interval -1.05V - +1.1V, Fig. 3b), focus on the region containing the supposed UPD peak. Identifying the onset of hydrogen electrosorption and the end of desorption as above, the net charge transferred during the corresponding H electrosorption process is found as $\delta Q_H = 0.7 \pm 0.05$ C. If this charge is converted into monolayers of adsorbed H using the value, 15.3 atoms/nm^2, of dense-packed Pd surfaces and a valency of 1, we estimate the covered surface area at 0.29 ± 0.02m^2. In view of the sample mass of 27.1mg, this would correspond to $\alpha_m = 10.6 \pm 0.8$ m^2/g, four times smaller than the α_m value estimated from the x-ray data. Thus, even if we account for the presence of sinter necks at the contact between adjacent particles and for the ensuing reduction in area accessible to electrolyte, we must conclude that the amount of adsorbed H in the cycles of Fig. 3b) is not sufficient to form a full UPD monolayer.

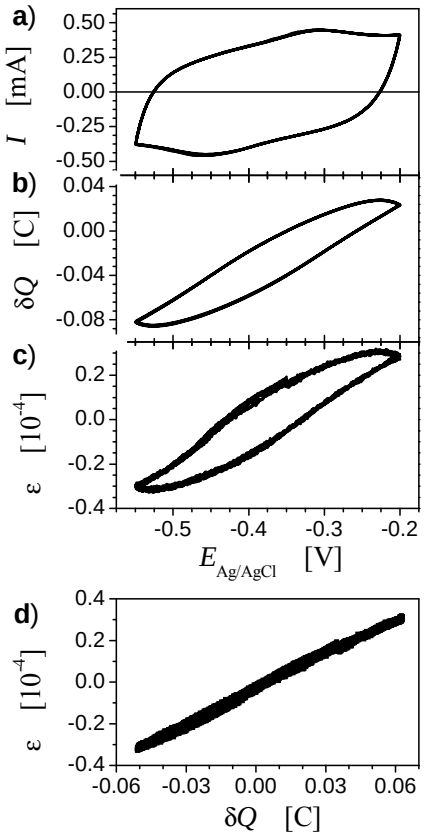

Figure 4. Results of in-situ dilatometry studies of pnc-Pd in NaF (0.7 M) electrolyte measured in the double layer interval –0.55V < E > –0.2 V. Scan rate: 1 mV/s. (a) Cyclic scans of current I vs. potential E. (b) Net charge transfer δQ vs. E. (c) Strain ε vs. E. (d) ε vs. the charge transfer δQ. The potential at which $\delta Q = 0$ is chosen arbitrary.

The above conclusion can be verified by inspecting the surface area from the point of view of oxygen species adsorption. Here, the net charge is 2.0±0.07 C, and a lower bound for the active surface area is obtained by assuming that 1 ML of neutral oxygen is adsorbed, at 2 electrons per OH^- ion. The result is 15.1±0.5 m^2/g, still larger than the maximum area that can be covered by a full ML of H in view of the voltammetric charge in the H electrosorption region.

The above considerations on the net surface area are significant inasmuch as they confirm that the amount of H adsorbed in the scans of Fig. 3 corresponds to less than a full monolayer on the sample surface. This is consistent with the identification of the associated peak in the CV with H UPD, and it supports our discussion, see below, of the strain signal during the early stages of H electrosorption in terms of the electrocapillary response of the Pd surface to H adsorption.

Electrocapillary response

Under the assumption that bulk concentration changes are negligible, the strain in response to potential changes can be attributed to the action of the surface stress [12]. Changes in the surface charge density, q, change f and thereby lead to expansion or contraction of the macroscopic sample. The relevant materials parameter of the surface is the electrocapillary coupling parameter ς.

By using the mass-specific surface area, α_m, the variation δf in the mean surface stress relative to an arbitrary reference state can be determined from the macroscopic strain, ε, via [12]

$$\delta f = -\frac{9\,K}{2\,\alpha_m\,\rho}\delta\varepsilon\,. \qquad (2)$$

The symbols have the following meaning: K - bulk modulus of the solid phase, ρ – mass density of the solid phase. In view of Eq (1) we may take, for any given electrode process, $\delta f = \varsigma\,\delta q$. Since $q = Q/A$ and $A = m\,\alpha_m$ with m the sample mass, the electrocapillary coupling parameter is then obtained from the data as

$$\varsigma = -\frac{9\,K\,m}{2\,\rho}\frac{\delta\varepsilon}{\delta Q}\,. \qquad (3)$$

It is seen that electrocapillary coupling can be measured independent of α_m, so that the uncertainty in the specific surface area does not propagate into the computation of ς [12].

When rearranged as

$$-\frac{9\,K\,m}{2\,\rho}\delta\varepsilon = \varsigma\,\delta Q\,, \qquad (4)$$

Eq. (3) can be exploited to determine ς from the data for strain versus charge from Figs. 2-4. To this end we plot, in Fig. 5, the left-hand side of Eq (4) versus δQ, noting that here $(-9\,K\,m)/(2\rho)$ takes on the value -1.90kJ. In the representation of Fig. 5, the slopes of the graphs provide immediately the coupling parameter ς.

The evaluation of ς is straightforward for the regime of capacitive charging (Fig. 4 and Fig. 5a)). The graph in Fig. 5a) is nearly straight, and the slope of the straight line of best fit gives ς = - 1.07±0.07 V. This is considerably smaller than the value, -2.0 V, found experimentally for ς on clean 111-textured Au surfaces [37], yet almost identical to the -1.06 V found for capacitive charging of pnc-Pt [19]. The finding may also be compared with a recent density functional theory (DFT) study of electrocapillary coupling of various transition and noble metals [39]. That study predicts the value of ς for capacitively charged Pd (111) surfaces to agree closely with Pt and to be about half the value for the corresponding Au surfaces. The agreement of these findings with the experiment is apparent, and specifically the present value of ς = -1.07±0.07 V is very close to the DFT-result of Ref. [39] for Pd (111), ς = -0.98 V.

The regime of oxygen species electrosorption is best resolved in the data of Figs. 3 and their representation in 5b). Fits in the initial regime (δQ < 1.5 C in Fig. 5b)) yield ς = -0.86±0.15 V for oxygen species electrosorption. Again, this agrees with experiments on Pt, where the corresponding ς-value is 0.8±0.1 V [19].

Before moving on to the discussion of the potential-strain response during H electrosorption, we investigate the mechanics of solute incorporation into the bulk and near the surface of an elastic nanoparticle.

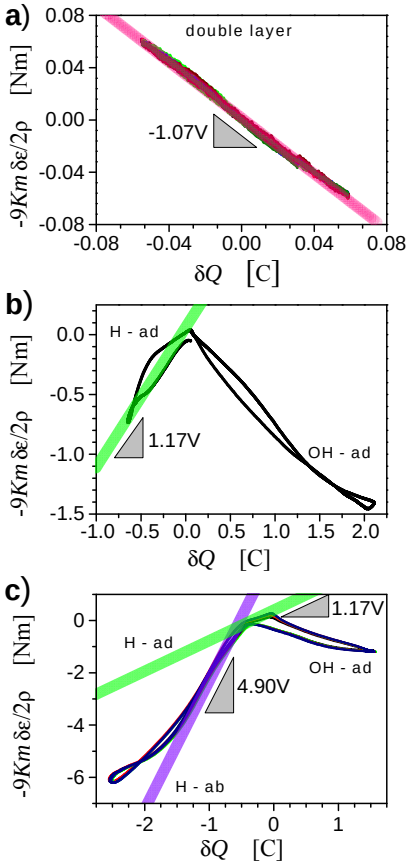

Figure 5. True and apparent electrocapillary coupling coefficients, ς. Motivated by Eq (4), thin lines shows $-9Km\,\delta\varepsilon/2\rho$ versus δQ for scans in different potential intervals, with data in subfigures **a)**, **b)**, and **c)** computed from dilatometry data of Figures 4, 3, and 2, respectively. Slope of thick semitransparent straight lines provide value of ς, as indicated by values annotating the triangles. In a), ς is obtained from a straight-line fit (red line) to the data. In b) and c), ς is from theory, Eq. (10) for H adsorption (green lines) and Eq. (7) for H absorption (blue line). States with zero abscissa and ordinate values are chosen arbitrarily.

A model for sorption strain

As a simple model (Fig. 6), let us consider the absorption of a misfitting interstitial solute atom in the bulk, focusing on the limiting case where the surface processes are rate limiting and diffusion is sufficiently fast for the solute to be distributed homogeneously throughout the bulk of each nanoparticle. This is motivated by the almost instantaneous equilibration of H in nanoparticles: The diffusion coefficient, D, of H in bulk Pd at T = 298 K has been reported as 3.8 x 10^{-11} m^2/s [40, 41]. Estimating the diffusion distance at $\sqrt{Dt}$, the time required for diffusing hydrogen from the surface to the centre of a 10 nm particle is obtained as 3 μs, orders of magnitude shorter than the experiment.

For uniform hydrogen concentration each grain strains uniformly and isotropically, with the lattice parameter, a, related to that of pure Pd, a_0, by

$$a = a_0 (1 + \eta x) . \qquad (5)$$

Here x denotes the H fraction (H atoms per Pd atoms) and η a concentration strain coefficient, of magnitude $\eta = 0.063$ [42]. In situ diffraction experiments on nanocystalline porous samples with a granular microstructure similar to the present ones have shown that the dilatometry signal agrees with the lattice parameter change [12], in other words, $\delta\varepsilon = \delta a/a_0 = \eta\, \delta x$. It is therefore straightforward to predict the macroscopic strain due to a given amount of charge transfer, δQ, when 1 electron is transferred per H absorbed. The result is

$$\delta\varepsilon = -\frac{\eta \rho \Omega}{m\, q_0} \delta Q \ . \qquad (6)$$

with Ω the atomic volume of Pd and q_0 the elementary charge. If the data was used – inappropriately – to determine an electrocapillary coupling parameter by means of Eq. (3), then the apparent value of ς during H absorption in bulk would be

$$\varsigma_{ab}^{\text{apparent}} = \frac{9 K \eta \Omega}{2\, q_0} \ , \qquad (7)$$

as is seen by inserting Eq. (6) into Eq. (3). The numerical value of the apparent ς is obtained as +4.9V. Materials parameters for Pd are K = 187 GPa, $\eta = 0.063$, $\Omega = 0.0147\text{nm}^3$ (see references in [31]).

Next, we consider the case where H is exclusively located in a thin layer at or near the surface. In the sense of Gibbs phenomenological thermodynamics, the scenario can be discussed in terms of generalized adsorption of an excess, Γ, of H per area. This holds even if the incorporation is not in surface sites but rather in a subsurface layer, provided that it represents a net amount of excess H in the solid at equilibrium that scales with the area of surface. If such a layer is thin enough, so that its volume is a negligible fraction of the net volume of a grain, then the grain acts as a rigid substrate which, to first approximation in surface area per (total) volume, suppresses strain in the tangent plane. Lemier and Weissmüller [31] have investigated that scenario with reference to H at grain boundaries in polycrystals and have found that it leads to an effective surface stress change of magnitude

$$\delta f_{\text{apparent}} = -\frac{Y}{1-\nu} \eta \Omega \Gamma \ , \qquad (8)$$

with Y the Young modulus and ν Poisson's ratio. By means of Eq. (2) this is seen to give rise to an isotropic strain of the grain interior, of magnitude

$$\varepsilon = \frac{2}{3} \frac{1-2\nu}{1-\nu} \alpha_m \eta \rho \Omega \Gamma \ , \qquad (9)$$

where it was used that, for isotropic solids, the elastic constants are related via $Y = 3K(1\text{-}2\nu)$. When we finally express Γ in terms of the associated charge density via $\Gamma = -q/q_0$, we obtain as the apparent electrocapillary coupling parameter for H adsorption at the surface

$$\varsigma_{ad} = \frac{3 K \eta \Omega}{q_0} \frac{1-2\nu}{1-\nu} \ . \qquad (10)$$

By comparison to Eq. (7) it is seen that the electrocapillary response is here less than the apparent value for H incorporation into the bulk of the solid. The reduction is by the factor $2(1\text{-}2\nu)/(3(1\text{-}\nu))$. By using $\nu = 0.34$ [43,44] and the materials parameters introduced above for H in Pd, we find the apparent ς as +1.17V, fourfold less than the apparent ς for bulk H absorption, Eq. (7).

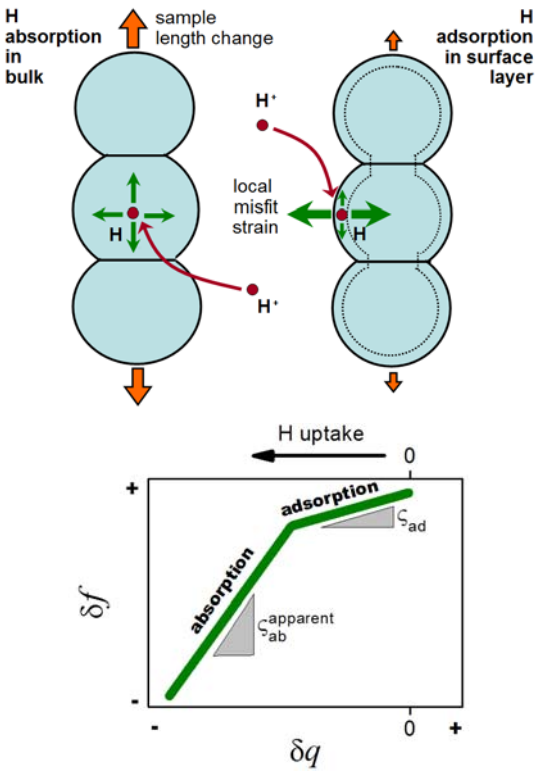

Figure 6 Schematic illustration of mechanical deformation of a chain of nanoparticles due to hydrogen incorporation into the bulk (top left) or in a layer near the surface (top right). The external strain sensed by a dilatometer is only dependent on the displacements that are propagating along the chain, whereas outward displacement of sections of the free surface are irrelevant. The former is larger for absorption in bulk. Bottom graph is a schematic of apparent variation of surface stress, f, with charge, q, per surface area. The two processes lead to different (apparent) electrocapillary coupling parameters, ς, as indicated in the figure and parameterized by the slopes of the graph of $f(q)$, green line . The transition occurs when the surface layers are saturated with hydrogen. Top ordinate indicates relation of q to uptake of hydrogen by electrosorption.

As is illustrated schematically in Fig. 6, the considerations so far highlight a difference in the macroscopic strain of the porous solid per charge – and, hence, per H atom – depending on where the H is dissolved: H in the bulk produces roughly four times more macroscopic strain than H at the surface. This was found even though the partial molar volume of H has the identical value, $3\eta\Omega$, in each case. In other words, the net volume change of the metal is independent of the location of the extra solute. The apparent contradiction is resolved when it is recognized that incorporating misfitting solute – such as H – at the surface results in an anisotropic strain field, with an outward displacement, or "stretch" [31], of the outermost layer of atoms as its dominant effect. Stretch reduces the pore volume but does not propagate along the network of

solid nanoparticles. By contrast, H in the bulk produces an isotropic strain field, which is more efficient in elongating the chains of nanoparticles that make up the backbone of the porous material. The above-mentioned distinction between the volume changes of the solid phase and of the macroscopic porous body had been recognized in earlier work [45] and confirmed by dedicated atomistic study [46] and experiments [47].

Comparing model and experiment

The results of Figs. 5b) and c) allow the true and apparent electrocapillary response for hydrogen electrosorption at the surface and in the bulk to be examined from an experimental point of view. For illustration we have included the prediction of the model as solid lines. The slopes of those lines represent the ς-values of Eqs (7) and (10), while their displacement along the ordinate is chosen for agreement with the experiment. It is seen, that the apparent break in the experimental graphs suggests a transition between adsorption and absorption at the value of $\delta Q \sim -0.6$ C in the scale of Fig. 5c). The model graph therefore represents a scenario where H is initially *adsorbed* up to a particular maximum value, Γ_{max}, of the specific excess, and then *absorbed* into the bulk. We cannot determine Γ_{max} because of the experimental uncertainty in the specific surface area. Yet, the discussion has emphasized that $\delta Q \sim -0.6$ C does represent a superficial excess of less than 1 atomic monolayer of H.

By inspection of Figs. 5b) and c) it is seen that the model agrees with the essentials of the experiment. Specifically, the data confirm a marked transition between a small electrocapillary response in the initial stage of H electrosorption and a much larger apparent electrocapillary response at the later stages. In the initial stage of electrosorption, the agreement between experiment and model is seen to be quite precise, with the experimental graph in Fig. 5b) reproducing quantitatively the slope of the model. The same feature is also observable in the data, Fig. 5c), for the larger potential interval, where a small region of weak potential strain response precedes the entry into the regime of steep variation. In this steeper region, the experimental graph varies less than the model. Yet, the qualitative difference between the two regimes is well reproduced.

The agreement in the initial stage of H electrosorption confirms the notion that this stage represents H UPD. The model value of $\varsigma = +1.17$ V is not inconsistent with the data from the shift of the UPD potential of strained Pd layers, $\varsigma = +1.4$ V, as reported in Ref. [18]. The present finding for Pd is also comparable to the experimental data for potential-strain response of pnc-Pt during H UPD, $\varsigma = +1.5$ V [19]. Here again there is at least qualitative agreement with DFT studies, since data in Ref. [17] imply $\varsigma = +1.9$ V for H adsorption on Pt (111) [18].

The transition to a much larger apparent electrocapillary response at the later stages of H electrosorption confirms the scenario developed in the model.

Conclusion

The results of in this in-situ dilatometry study of the deformation of porous nanocrystalline (pnc-) Pd in electrolyte can be summarized as follows:

Changes in the surface stress, *f*, during the electrosorption of hydrogen or of oxygen species on pnc-Pd induce large macroscopic strain that is readily measured by dilatometry. The surface stress response can be quantified by means of the electrocapillary coupling parameter, ς, defined as the derivative of *f* with respect to the superficial charge density.

By suitable selection of the intervals of electrode potential one can distinguish four different regimes, each with its own, characteristic value of ς. These regimes are oxygen species adsorption, capacitive charging of the electrochemical double-layer, hydrogen adsorption in the surface regions, and hydrogen absorption in the bulk.

Our results for ς during capacitive charging are well consistent with experiment on Pt and with DFT-data for Pd. The present results for ς during H adsorption support previous findings, derived more indirectly from the variation of the H electrosorption potential with tangential strain on Pd surfaces in epitaxy with substrates of different lattice parameters.

The values of ς differ strongly between H adsorption and absorption, and the difference can be quantitatively understood in terms of a model based on the continuum mechanics of superficial layers containing misfitting solute. The model considers H within the bulk of a thin layer. Its success might therefore indicate that adsorbed H here occupies subsurface sites. Yet, as we have exposed, H adsorption on the surface (and not in subsurface sites) of Pt gives a similar response to what is found for Pd. This might indicate a more general trend, where the elastic interaction of the solute with the surface is only weakly dependent on whether surface or subsurface sites are occupied. Our model might then represent a more general picture of the impact of adsorption on the capillary forces at solid surfaces.

Acknowledgment

RNV acknowledges the Department of Science and Technology, Government of India, for financial support under the Ramanujan Fellowship award.

References

[1] Weissmüller J, Cahn JW. Acta Mater 1997;45:1899.

[2] Michels D, Krill CE, Birringer R. J Magn Magn Mater 2002;250:203.

[3] Weissmüller J, Lemier C. Phil Mag Lett 2000;80:411.

[4] Diao JK, Gall K, Dunn ML. Phys Rev B 2004;70: 075413.

[5] Parida S, Kramer D, Volkert CA, Rösner H, Erlebacher J, Weissmüller J. Phys Rev Lett 2006;97: 035504.

[6] Farkas D, Crowson DA, Corcoran SG. Scripta Mater 2009; 61:497.

[7] Ibach H. Surf Sci Rep 1997;29:193.

[8] Haiss W. Rep Prog Phys 2001;64:591.

[9] R. Raiteri, M. Grattarola, H. J. Butt, and P. Skladal, Sensors Actuators B 79 (2001) 115.

[10] F. M. Battiston, J. P. Ramseyer, H. P. Lang, M. K. Baller, C. Gerber, J. K. Gimzewski, E. Meyer, and H. J. Güntherodt, Sensors Actuators B 77 (2001) 122.

[11] N. V. Lavrik, M. J. Sepaniak, and P. G. Datskos, Rev. Scient. Instr. 75 (2004) 2229.

[12] Weissmüller J, Viswanath RN, Kramer D, Zimmer P, Würschum R, Gleiter H. Science 2003;300**:**312.

[13] Kramer D, Viswanath RN, Weissmüller J. Nano Lett . 2004;4:793.

[14] Jin HJ, Wang XL, Parida S, Wang K, Seo M, Weissmüller J. Nano Lett 2010;10:187.

[15] Biener J, Wittstock A, Zepeda-Ruiz LA, Biener MM, Zielasek V, Kramer D, Viswanath R.N, Weissmüller J, Bäumer M, Hamza AV. Nature Mat 2009; 8:47.

[16] Umeno Y, Elsässer C, Meyer B, Gumbsch P, Nothacker M, Weissmüller J, Evers F. Europhys Lett 2007;78:13001.

[17] Feibelman PJ. Phys Rev B 1997;56:2175.

[18] Weissmüller J, Viswanath RN, Kibler LA, Kolb DM. Phys Chem Chem Phys 2011;13: 2114.

[19] Viswanath RN, Kramer D, Weissmüller J. Electrochim Acta 2008;53:2757.

[20] Mavrikakis M, Hammer B, Nørskov JK. Phys Rev Lett 1998;81:2819.

[21] Shao M, Liu P, Zhang J, Adzic R. J Phys Chem B 2007;111: 6772.

[22] Kibler LA, El-Aziz AM, Hoyer R, Kolb DM. Angew Chemie Int Edt 2005;44:2080.

[23] Strasser P, Koh S, Anniyev T, Greeley J, More K, Yu CF, Liu ZC, Kaya S, Nordlund D, Ogasawara H, Toney MF, Nilsson A. Nature Chem 2010; 2:454.

[24] Stafford GR, Bertocci U. J Phys Chem C 2009;113:13249.

[25] Iyer RN, Pickering HW. Annu Rev Mater Sci 1990;20:299.

[26] Flanagan TB, Oates WA. Annu Rev Mater. Sci. 1991;21: 269.

[27] Mütschele T, Kirchheim R. Scripta Metallur 1987;21:1101.

[28] Pundt A. Adv Eng Materials 2004;6:11.

[29] Pundt A, Sachs C, Winter M, Reetz MT, Fritsch D, Kirchheim R. J Alloys Comp 1999;480:293.

[30] Pundt A, Kirchheim R. Annu Rev Mater Res 2006;36:555.

[31] Lemier C, Weissmüller J. Acta Materialia 2007;55:1241.

[32] Gleiter H. Prog in Mat Sci 1989;33:233.

[33] Ames M, Markmann J, Karos R, Michels A, Tschöpe A, Birringer R. Acta Mater 2008;56:4255.

[34] Markmann J, Yamakov V, Weissmüller J. Scripta Mater 2008;59:15.

[35] Viswanath RN, Kramer D, Weissmüller J, Langmuir 2005;21:4604.

[36] El-Aziz AM, Kibler LA. J Electroanal. Chem. 2002;534: 107.

[37] Smetanin M, Viswanath RN, Kramer D, Beckmann D, Koch T, Kibler LA, Kolb DM, Weissmüller J. Langmuir 2008;24: 8561.

[38] Haiss W, Nichlos RJ, Sass JK, Charle K. J Electroanal Chem 1998;452:199.

[39] Albina JM, Elsässer C, Weissmüller J, Gumbsch P, Umeno Y. Phys Rev B 2012;85:125118.

[40] Wicke E, Brodowsky H. Hydrogen in Metals. Eds. Alefeld G, Völkel J. Berlin: Springer Verlag; pp. 73-155, 1978.

[41] Flanagam TB, Oates WA. Annu Rev Mater Sci 1991;21: 269.

[42] Baranowski B, Majchrzak S, Flanagan TB. J Phys F:Metal Phys 1971;1:258.

[43] Brandes EA, Brook GB. Editors, Smithells Metals Reference Book. Oxford: Butterworth-Heinemann; 1992.

[44] Köster W. Z Metallkunde 1949;39:111.

[45] Jin HJ, Parida S, Kramer D, Weissmüller J, Sur Sci 2008;602:3588.

[46] Weissmüller J, Duan HL, Farkas D. Acta .Mater 2010;58: 1.

[47] Shao LH, Jin HJ, Viswanath RN, Weissmüller J. Europhys Lett 2010;89:66001.